

## TRANSIENT MAGNETOHYDRODYNAMIC FLOW OF EYRING-POWELL FLUID IN A POROUS MEDIUM

Oyelami, F.H.<sup>1,2</sup> and Dada, M.S.<sup>2</sup>

<sup>1</sup>Department of Mathematical and Physical Sciences, Afe Babalola University, Ado Ekiti, Nigeria

<sup>2</sup>Department of Mathematics, University of Ilorin, Ilorin, Nigeria  
Corresponding Author: adefolajufunmilayo@gmail.com

(Received: 14<sup>th</sup> Aug., 2015; Accepted: 16<sup>th</sup> May, 2016)

### ABSTRACT

This study investigated the effects of magnetic field, thermal radiation and viscous dissipation on transient magneto hydrodynamic (MHD) flow of non-Newtonian incompressible fluid obeying Eyring-Powell model in a porous medium. The governing equations were formulated and transformed into non-dimensional equations. Numerical solution to the transformed governing nonlinear partial differential equations was obtained using the implicit finite difference scheme of Crank-Nicolson type. The finite difference equations form Thomas algorithm tri-diagonal matrix system of equations which was solved using the MATLAB. The results showed that a rise in Non-Newtonian parameter  $F$ , thermal Grashof number  $Gr$ , modified Grashof number  $Gm$  and dissipation function  $Ec$ , caused velocity to increase whereas velocity decreased with increase in Non-Newtonian parameter  $A$ , magnetic field parameter  $M$ , radiation parameter  $R$ , Schmidt number  $Sc$ , Prandtl Number  $Pr$  and chemical reaction parameter,  $\gamma$ . Temperature increased with increase in dissipation function  $Ec$ , while it decreased as Prandtl number, magnetic field parameter and Radiation number increased. Increase in Schmidt number and chemical reaction result to a decrease in concentration.

**Keywords:** Non-Newtonian; Radiation; Magnetic Field; Eyring-Powell Model; Dissipation.

### INTRODUCTION

Fluid can be regarded as a material in nature that deforms continually under applied shear stress. The most important property of fluid that characterizes the flow resistance of simple fluids is its viscosity. It is the ratio of shear stress to the shear strain. Shear stress is known to be a measure of the force of friction from a fluid acting on a body in the path of that fluid while shear strain measures the changes in angle with respect to two specific directions. The viscous behaviour of fluids depends on the relationship between shear stress and rate of deformation. Some fluids exhibit linear relationship between shear stress and rate of deformation while some are non-linear in nature. Those that exhibit linear relationship are referred to as Newtonian fluid (water, air and benzene).

Another very important type of fluid which is different from Newtonian fluid is the one that does not exhibit linear relationship between shear stress and the rate of deformation. Such fluids are referred to as Non-Newtonian fluids (inks, glues, polymer solutions, gel, and coal-water). A good description of this fluid is given by Bird *et al.*

(1960). Non-Newtonian fluids are of great importance in manufacturing and chemical industries due to their numerous applications in drilling for petroleum, extrusion of polymer, molding of metal substances and blasting of glasses. In the area of modeling flow of fluids in porous medium, heat transfer analysis has always been of interest. As a result of this, control measure is very important for rate of heat transfer in manufacturing industries for quality control and reduction of thermal radiation and its emissions to the body (Adesanya and Gbadeyan, 2011). The viscous behaviour (non-linear) of non-Newtonian fluids can be analyzed using several models. The models are power law model, Eyring-Powell model, Eyring-Prandtl model, Cross model, Yasuda model and Bingham (Darji and Timol, 2013).

Literature on non-Newtonian fluids are rare because of the complexity of these models. The few that are available use Power-law model because the rheological features of Power-law can only be captured by a single constitutive relationship between shear stress and rate of deformation (shear strain). An advantage of

Eyring-Powell model over Power-law model is that it correctly reduces to Newtonian behaviour for low and high shear rate. The Eyring-Powell model, according to Mansutti *et al.* (1993); Manisha and Timol, (2009) can be defined as:

$$\tau_{xy} = \mu \frac{\partial u}{\partial y} + \frac{1}{\alpha} \sinh^{-1} \left( \frac{1}{c} \frac{\partial u}{\partial y} \right) \quad (1)$$

where  $\tau_{xy}$  is the shear stress  $\frac{\partial u}{\partial y}$  is the velocity gradient,  $\mu$  is the coefficient of dynamic viscosity,  $\alpha$  and  $c$  characterize the Eyring-Powell fluid model.

Numerous practical applications and studies have brought about considerable interest in studying the flow of Non-Newtonian fluids. Islam *et al.* (2009), Patel and Timol (2009), Patel and Timol (2011) and Hayat *et al.* (2012) used Eyring-Powell model to analyze viscous behavior of non-Newtonian fluids. Eldabe *et al.* (2003) investigated the non-Newtonian fluid flow under the effect of couple stresses between two parallel plates using Eyring-Powell model. The authors found out that increase in the degree of Taylor polynomial increases the maximum absolute error. Numerical study of viscous dissipation effect on free convection heat and mass transfer of magneto hydrodynamic (MHD) non-Newtonian fluid flow through a porous medium was carried out by Nabil *et al.* (2012). The numerical results indicated that as the non-Newtonian and magnetic parameters increase, the value of the velocity decreases. The authors conclusion met the logic of the magnetic field exerting a retarding force on the free convection flow with effect of thermal radiation being considered on the free convection heat and mass transfer of magneto hydrodynamic (MHD) non-Newtonian fluid. Malik *et al.* (2013) obtained boundary layer flow of an Eyring-Powell model fluid due to a stretching cylinder with a variable viscosity. Their analytical solution was obtained using homotopic analysis and the result showed that thermal boundary layer decreases with increased Prandtl and Reynold numbers. The effect of viscous dissipation and thermal radiation on fluid behavior was not studied. Radiation effects on boundary layer flow of an Eyring-Powell fluid over an exponentially shrinking sheet was investigated by Asmat *et al.* (2014). Using homotopy analysis, it was observed that velocity increases with an increase in mass suction and the thermal boundary layer thickness decreases due to increase in Prandtl number and

thermal radiation. However, magnetic field effect and viscous dissipation were not considered. Tasawar *et al.* (2014) investigated the radiation effects on the flow of Powell-Eyring fluid past an unsteady inclined stretching sheet with non-uniform heat source/sink. The study addressed the radiation effects and established that velocity increased with increase in radiation while the temperature decreased. The effect of viscous dissipation was however neglected. Darji and Timol (2013) investigated group theoretical similarity analysis for natural convection boundary layer flow of a class of non-Newtonian fluids. It was observed in their work that the velocity in Williamson model was higher than that of Prandtl-Eyring model. The Adomian decomposition approach to visco-elastic fluid flow with slip through a planer channel was studied by Adesanya and Gbadeyan (2011). The combined effect of Navier slip and magnetic field was investigated on the radiative heat transfer of a steady flow of a conducting, viscous, non-Newtonian and incompressible fluid through a channel filled with saturated porous medium. It was observed that the effect of porosity parameter was to reduce the velocity whereas increasing the Grashof number increased the velocity of the fluid. Adesanya and Gbadeyan (2011), Gbadeyan and Dada (2013) investigated the influence of radiation and heat transfer on an unsteady MHD Non-Newtonian fluid flow with slip in a porous medium in which the effect of magnetic field and thermal radiation was considered. However, the effect of viscous dissipation and the presence of chemical reaction was not considered. In previous studies and researches, the combined effects of magnetic field, viscous dissipation and thermal radiation were neglected, while heat and mass transfer with effect of viscous dissipation in non-Newtonian flow of Eyring-Powell fluids is comparatively less well-known.

Consequently, this study therefore investigated the combined effects of magnetic field, thermal radiation and viscous dissipation on the transient magneto hydrodynamic flow of non-Newtonian incompressible fluid obeying Eyring-Powell model. The governing equations were formulated and transformed to non-dimensional equations. Numerical solution to the transformed governing nonlinear partial differential equations was

obtained using the implicit finite difference scheme of Crank-Nicolson type. The finite difference equations form Thomas algorithm tri-diagonal matrix system of equations, which was solved using MATLAB. The physical parameters arising from the flow were studied on velocity, temperature and concentration profiles. Variations of these parameters that affect the flow were also studied on the skin friction, Nusselt and Sherwood numbers.

**FORMULATION OF THE PROBLEM**

Transient free convection incompressible electrically conducting non-Newtonian Eyring-Powell fluid between two vertical parallel plates in a saturated porous medium situated at distance h apart was considered. The x\* - axis was taken along the plate while the y\* - axis was taken normal to it in the fluid. Along y\*- axis in the fluid flow, a magnetic field of uniform strength was applied. The medium was porous and homogeneous chemical reaction of the first order was assumed to be present. Both wall temperatures T<sub>o</sub>\* and T<sub>w</sub>\* were high enough to induce thermal radiation. Taking into account the Boussineq approximations, the governing equations were formulated as follows.

$$\rho \frac{\partial u^*}{\partial t^*} = - \left( \frac{\partial p}{\partial x^*} - \frac{\partial T_{xy}}{\partial y^*} \right) + g\rho\beta(T^* - T_0^*) + g\rho\beta_c(C^* - C_0^*) + \sigma B_0^2 u^* - \frac{\mu u^*}{k} \quad (2)$$

$$\frac{\partial T^*}{\partial t^*} = \frac{k}{\rho c_p} \frac{\partial^2 T^*}{\partial y^{*2}} - \frac{1}{\rho c_p} \frac{\partial q_r}{\partial y^*} + \frac{\nu}{c_p} \left( \frac{\partial u^*}{\partial y^*} \right)^2 \quad (3)$$

$$\frac{\partial C^*}{\partial t^*} = D \frac{\partial^2 C^*}{\partial y^{*2}} - K_c(C_1^* - C_0^*) \quad (4)$$

The initial and boundary conditions are given as

$$\begin{aligned} t^* = 0, u^* = 0, T^* = T_0^*, C^* = C_0^*, y \in (0, h) \\ t^* > 0, u^* = \lambda \frac{\partial u^*}{\partial y^*}, T^* = T_0^*, C^* = C_0^* \text{ at } y^* = 0 \\ u^* = 0, T^* = T_1^*, C^* = C_1^* \text{ at } y^* = h \end{aligned} \quad (5)$$

where μ\* is the velocity of the fluid in the x- direction, t\* is the time, ρ is the density of the fluid, g is the acceleration due to gravity, T\* is the fluid temperature, C\* is the fluid

concentration, P is the fluid pressure, β is the coefficient of thermal expansion, K is the thermal conductivity, T<sub>w</sub>\* and C<sub>w</sub>\* are the temperature and concentration of the fluid at y\* = h, T<sub>o</sub>\* and C<sub>o</sub>\* are the temperature and concentration of the fluid at y\* = 0 D is the mass diffusivity q<sub>r</sub> is the radiative heat flux, σ is the electrical conductivity, υ is the kinematic viscosity, B<sub>o</sub> is the magnetic field, h is the distance between two plates, K<sub>c</sub> is the rate of chemical reaction and T<sub>xy</sub> is the Eyring-Powell non-Newtonian fluid stress tensor.

According to Manisha and Timol (2009), Malik *et al.* (2013) and Asmat *et al.* (2014), the Eyring-Powell model is defined as follows

$$T_{xy} = \mu \frac{\partial u^*}{\partial y^*} + \frac{1}{\alpha} \sinh^{-1} \left( \frac{1}{c} \frac{\partial u^*}{\partial y^*} \right) \quad (6)$$

where τ<sub>xy</sub> is the shear stress,  $\frac{\partial u}{\partial y}$  is the velocity gradient, μ is the coefficient of dynamic viscosity, α and c characterizes the Eyring-Powell fluid model.

Taking the first and second order approximation of the hyperbolic sine function gives

$$\sin h^{-1} \left( \frac{1}{c} \frac{\partial u^*}{\partial y^*} \right) \cong \frac{1}{c} \frac{\partial u^*}{\partial y^*} - \frac{1}{6} \left( \frac{1}{c} \frac{\partial u^*}{\partial y^*} \right)^3, \left| \frac{1}{c} \frac{\partial u^*}{\partial y^*} \right| \ll 1 \quad (7)$$

Hence the stress tensor for Eyring-Powell model becomes

$$T_{xy} = \mu \frac{\partial u^*}{\partial y^*} + \frac{1}{\alpha c} \left[ \frac{\partial u^*}{\partial y^*} - \frac{1}{6c^2} \left( \frac{\partial u^*}{\partial y^*} \right)^3 \right] \quad (8)$$

In the optically thin limit case, Cogley *et al.* (1968) showed that

$$\frac{\partial q_r}{\partial y^*} = 4(T^* - T_0^*) \int_0^\infty k\lambda_w \left( \frac{d e_{b\lambda}}{dT^*} \right)_w d\lambda \quad (9)$$

Where kλ<sub>w</sub> is the absorption coefficient and e<sub>bλ</sub> is the plank function, L =  $\int_0^\infty k\lambda_w \left( \frac{d e_{b\lambda}}{dT^*} \right)_w d\lambda$

Combining (8) and (9), the momentum and energy equations can be defined as follows:

$$\begin{aligned} \rho \frac{\partial u^*}{\partial t^*} - \frac{1}{\rho} \frac{\partial p^*}{\partial x^*} + \frac{\mu}{\rho} \frac{\partial^2 u^*}{\partial y^{*2}} + \\ \frac{1}{\rho \alpha c} \frac{\partial^2 u^*}{\partial y^{*2}} - \frac{1}{2\rho \alpha c^3} \left( \frac{\partial u^*}{\partial y^*} \right)^2 \frac{\partial^2 u^*}{\partial y^{*2}} \\ g\beta(T^* - T_0^*) + g\beta_c(C^* - C_0^*) + \sigma B_0^2 u^* - \frac{\nu u^*}{k} \end{aligned} \quad (10)$$

$$\frac{\partial T^*}{\partial t^*} = \frac{k}{\rho c_p} \frac{\partial^2 T^*}{\partial y^{*2}} - \frac{4L(T^* - T_0^*)}{Pr C_p} + \frac{v}{C_p} \left( \frac{\partial u^*}{\partial y^*} \right)^2 \quad (11)$$

Defining these non-dimensional quantities

$$x = \frac{x^* u_0^*}{v}, y = \frac{y^* u_0^*}{v}, u = \frac{u^*}{u_0^*}, t = \frac{t^* u_0^{*2}}{v}, \gamma = \frac{K_c v}{u_0^{*2}}, h = \frac{v}{u_0^*}, P = \frac{P^*}{\rho u_0^{*2}} \quad (12)$$

$$\frac{\partial T}{\partial t} = \frac{1}{Pr} \frac{\partial^2 T}{\partial y^2} - RT + Ec \left( \frac{\partial u^*}{\partial y^*} \right)^2 \quad (13)$$

$$\frac{\partial C}{\partial t} = \frac{1}{Sc} \frac{\partial^2 C}{\partial y^2} - \gamma C \quad (14)$$

where  $A = \frac{1}{\alpha \mu c}$  and  $F = \frac{u_0^{*4}}{2 \rho \alpha v^3 c^3}$  are the non-Newtonian parameters, the pressure gradient  $G$  is constant,  $u$  is the dimensionless velocity,  $t$  is the dimensionless time,  $T$  is the dimensionless temperature function,  $C$  is the dimensionless concentration function,  $R$  is the thermal radiation heat transfer parameter,  $Pr$  is the Prandtl number signifying the relative importance of heat conduction and viscosity of the fluid,  $Sc$  is the Schimidt number showing the ratio of momentum diffusivity and mass diffusivity,  $\gamma$  is the chemical reaction parameter,  $Da$  is the Darcy number showing the permeability of the porous medium,  $Re$  is the Reynold number,  $Gr$  is the thermal Grashof number giving the relative importance of buoyancy forces to viscous forces and  $Gm$  is the species Grashof number,  $M$  is the Magnetic field parameter,  $Ec$  is the Eckert number characterising the effect of dissipation.

With the corresponding dimensionless boundary conditions

$$\begin{aligned} t = 0, \quad u = 0, \quad T = 0, \quad C = 0, \quad y \in (0, h) \\ t > 0, \quad u = s_\lambda \frac{\partial u}{\partial y}, \quad T = 0, \quad C = 0 \quad \text{at } y = 0 \\ u = 0, \quad T = 1, \quad C = 1, \quad \text{at } y = 1 \end{aligned} \quad (15)$$

where  $s_\lambda = \frac{\lambda}{h}$  is the slip at the lower wall. For this type or flow, skin friction coefficient, local Nusselt and Sherwood numbers are of great importance. The dimensionless skin friction, Nusselt and Sherwood numbers are given as follows:

$$\tau = \left[ -\frac{\partial u}{\partial y} \right]_{y=0} \quad (16)$$

$$Nu = \left[ -\frac{\partial T}{\partial y} \right]_{y=0} \quad (17)$$

$$Sh = \left[ -\frac{\partial C}{\partial y} \right]_{y=0} \quad (18)$$

### SOLUTION TO THE PROBLEM

The set of nonlinear partial differential equations (12), (13) and (14) were solved by employing Crank Nicolson finite difference scheme. The equations are written in their discretized form as follows:

$$\begin{aligned} \frac{u_j^{k+1} - u_j^k}{\Delta t} = & \left[ 1 + A - F \left( \frac{u_{j+1}^k - u_{j-1}^k}{2\Delta y} \right)^2 \right] \left[ \frac{u_{j-1}^{k+1} - 2u_j^{k+1} + u_{j+1}^{k+1} + u_{j-1}^k - 2u_j^k + u_{j+1}^k}{2(\Delta y)^2} \right] + G_r \left( \frac{T_j^{k+1} + T_j^k}{2} \right) + G_m \left( \frac{C_j^{k+1} + C_j^k}{2} \right) + \left( M - \frac{Da}{Re^2} \right) \left( \frac{u_j^{k+1} + u_j^k}{2} \right) \end{aligned} \quad (19)$$

$$\begin{aligned} \frac{T_j^{k+1} - T_j^k}{\Delta t} = & \frac{1}{Pr} \left[ \frac{T_{j-1}^{k+1} - 2T_j^{k+1} + T_{j+1}^{k+1} + T_{j-1}^k - 2T_j^k + T_{j+1}^k}{2(\Delta y)^2} \right] - R \left[ \frac{T_j^{k+1} + T_j^k}{2} \right] + \frac{Ec}{4(\Delta y)^2} (u_{j+1}^k - u_{j-1}^k)^2 \end{aligned} \quad (20)$$

$$\frac{C_j^{k+1} - C_j^k}{\Delta t} = \frac{1}{Sc} \left[ \frac{C_{j-1}^{k+1} - 2C_j^{k+1} + C_{j+1}^{k+1} + C_{j-1}^k - 2C_j^k + C_{j+1}^k}{2(\Delta y)^2} \right] - \gamma \left[ \frac{C_j^{k+1} + C_j^k}{2} \right] \quad (21)$$

Let  $\left[ 1 + A - F \left( \frac{u_{j+1}^k - u_{j-1}^k}{2\Delta y} \right)^2 \right] = H_i$ , equation (18) becomes

$$\begin{aligned} \frac{u_j^{k+1} - u_j^k}{\Delta t} = & H_i \left[ \frac{u_{j-1}^{k+1} - 2u_j^{k+1} + u_{j+1}^{k+1} + u_{j-1}^k - 2u_j^k + u_{j+1}^k}{2(\Delta y)^2} \right] + G_r \left( \frac{T_j^{k+1} + T_j^k}{2} \right) + G_m \left( \frac{C_j^{k+1} + C_j^k}{2} \right) + \left( M - \frac{Da}{Re^2} \right) \left( \frac{u_j^{k+1} + u_j^k}{2} \right) \end{aligned} \quad (22)$$

With the following boundary conditions

$$u_j^{k+1} = 0, u_j^k = 0, T_j^{k+1} = 0, T_j^k = 0, C_j^{k+1} = 0, C_j^k = 0, \forall j, t = 0$$

$$u_{j-1}^{k+1} = \frac{-2\Delta y u_j^{k+1}}{s_\lambda} + u_{j+1}^{k+1}, T_{j-1}^{k+1} = 0, C_{j-1}^{k+1} = 0, j = 1, t > 0$$

$$u_{j-1}^k = \frac{-2\Delta y u_j^k}{s_\lambda} + u_{j+1}^k, T_{j-1}^k = 0, C_{j-1}^k = 0, j = 1, t > 0$$

$$u_j^{k+1} = 0, T_j^{k+1} = 1, C_j^{k+1} = 1, j = n, t > 0$$

$$u_j^k = 0, T_j^k = 1, C_j^k = 1, j = n, t > 0$$

Equations (20), (21) and (22) were multiplied by  $\Delta t$  for simplicity. The equations were now arranged such that momentum, energy and species equations at the present time step ( $k+1$ ) were on the left while those of previous time step ( $k$ ) were on the right hand side. Applying the equations to all nodes, a system with tri-diagonal matrix system of equations was obtained which can now be written as follows:

$$-A2u_{j-1}^{k+1} + B2u_j^{k+1} - C2u_{j+1}^{k+1} = F2$$

$$-A3T_{j-1}^{k+1} + B3T_j^{k+1} - C3T_{j+1}^{k+1} = F3$$

$$-A4C_{j-1}^{k+1} + B4C_j^{k+1} - C4C_{j+1}^{k+1} = F4$$

Where

$$A2 = E1, B2 = 1 + 2E1 - E2 + E3, C2 = E1, A3 = E6, B3 = 1 + 2E6 + E7, C3 = E6, A4 = E9,$$

$$B4=1+2E9+E10, C4=E9, F2=E1u_{j-1}^k + [1-2E1+E2-E3]u_j^k + E1$$

$$u_{j+1}^k + E4[T_j^{k+1} + T_j^k] + E5[C_j^{k+1} + C_j^k],$$

$$F3 = E6u_{j+1}^k + E4[T_j^{k+1} + T_j^k] + E5[C_j^{k+1} + C_j^k]$$

$$F4 = E9 C_{j+1}^k + [1 - 2E9 - E10]C_j^k + E9C_{j+1}^k$$

And  $E1 = \frac{\Delta t H_i}{2(\Delta y)^2}, E2 = \frac{M \Delta t}{2},$

$$E3 = \frac{Da \Delta t}{2(Re)^2}, E4 = \frac{\Delta t Gr}{2}, E5 = \frac{\Delta t Gm}{2}, E6 = \frac{\Delta t}{2Pr(\Delta y)^2}$$

$$E7 = \frac{R \Delta t}{2}, E8 = \frac{Ec \Delta t}{4(\Delta y)^2}, E9 = \frac{\Delta t}{2Sc(\Delta y)^2}, E10 = \frac{\gamma \Delta t}{2}$$

The computations were carried out by using subscripts  $j$  and  $k$  as the grid points along  $y$  and  $t$  direction. Initial conditions were used to solve for the values of  $u, T$  and  $C$  at all grid points. The values gotten at the previous time ( $k$ ) level was used at time ( $k + 1$ ) level to calculate the values of  $u, T$  and  $C$  as follows:

Equation (25) on a given  $j$ -level at every internal nodal point forms a tri-diagonal system of equation. Thomas algorithm which was discussed in Carnahan *et al.* (1969) was used to provide solution to the problem. With this, the value of  $C$  on a given  $j$ -level at time ( $k + 1$ ) level was known at every nodal point. Also, the values of  $T$  and  $C$  at time ( $k + 1$ ) level were calculated using equation (24). The results of  $T$  and  $C$  at time ( $k + 1$ ) level were used in equation (23) to calculate  $u$  at time ( $k + 1$ ) level.

Hence, the values of  $C, T$  and  $u$  were known at a particular  $j$ -level. This process was carried out several times at various  $j$ -level. This way, the values of  $C, T$  and  $u$  were known at all grid point. The following discussion was carried out for different values of the non-Newtonian parameters  $A$  and  $F$ , Prandtl number  $Pr$ , thermal Radiation parameter  $R$ , thermal Grashof number  $Gr$ , species Grashof number  $Gm$ , permeability parameter  $Da$ , Eckert number for dissipation function, Schmidt number, Magnetic field parameter  $M$  and the chemical reaction parameter  $\gamma$ . Default values for the  $C$  parameters are given as follows:

$$Pr = 0.76, Gr = 15, Gm = 15, M = 1.0, A = 20, F = 0.05, Re = 1.0, R = 1.0, Da = 0.1, \gamma = 1, s_\lambda = 1.$$

It should be noted that all graphs correspond to these values except stated otherwise on the graph.

### RESULTS AND DISCUSSION

Figure 1 presents the velocity distribution for various values of non-Newtonian parameter  $A$ . It was discovered that parameter  $A$  causes reduction in flow rate of the non-Newtonian fluid, Hence it reduces the velocity distribution. Figure 2 illustrates the effect of non-Newtonian parameter  $F$  on the velocity distribution. On this profile, increase in parameter  $F$  causes a rise in velocity distribution. However, from Figures 1 and 2, it can be concluded that the low rate of flow experienced in non-Newtonian fluid is caused by parameter  $A$ .

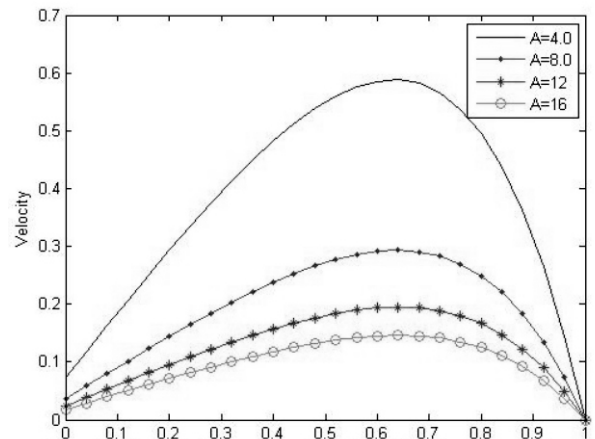


Figure 1: Velocity Profile for various values of Non Newtonian Parameter A at t=1

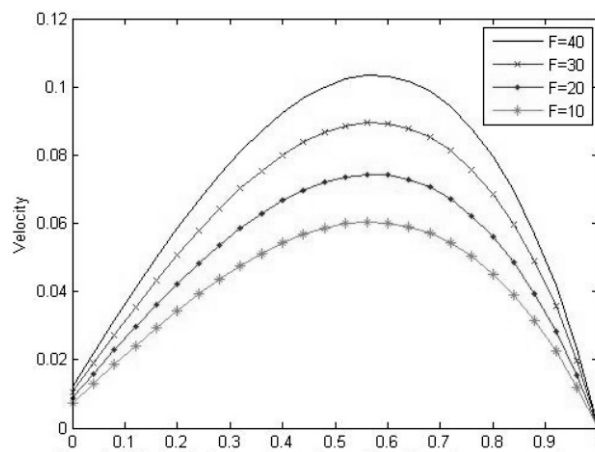


Figure 2: Velocity Profile for various values of Non-Newtonian parameter F at t=1

Figure 3 illustrates the velocity distribution for various values of thermal Grashof number  $Gr$ . An increase in  $Gr$  causes the velocity distribution to increase as this increase boost the buoyancy force. Figure 4 shows the influence of Magnetic field  $M$  on the velocity distribution. It was observed that the presence of  $M$  in an electrically conducting fluid give rise to an increase in Lorentz force that causes a retardation in the motion of fluid. An increase in  $M$  therefore reduces the velocity distribution. The effects of species Grashof number  $G_m$  is shown in Figure 5. It was observed that increase in species Grashof number  $G_m$  causes the velocity profile to increase. Figures 6 and 7 show the effect of Radiation and Darcy number on the velocity profile. Radiation parameter reduces the velocity profile and this reduction in velocity is accompanied by reduction in velocity layers while Darcy number decreases the velocity profile, thereby decreasing the permeability of the medium. Figures 8 and 9 show the influence of dissipation parameter ( $Ec$ ) and Schmidt number on the velocity profile. The work of the dissipation function  $Ec$  is to accelerate energy in the fluid motion thereby increasing the buoyancy force which is evident in Figure 8. As  $Ec$  increases, an increase in the velocity profile was observed while  $Sc$  reduces the velocity profile.

In Figure 13, decrease in the velocity profile for variations of Prandtl number was observed. The influence of Prandtl number  $Pr$  and Radiation Parameter  $R$  on the temperature profile is shown in on Figures 14 and 15 respectively. Increase in Prandtl number causes the thermal condition to decrease, this decrease was experienced because smaller value of  $Pr$  increases the thermal conductivity of the fluid temperature. As  $R$  increases, significant fall in the temperature profile is experienced. This is because, higher values of radiation term corresponds to smaller radiation flux and as a result, thermal radiation reduces the rate of energy transport to the fluid. Figure 16 shows the effect of dissipation function  $Ec$  on the temperature profile. As  $Ec$  increases,

temperature profile decreases. The effects of increasing Schmidt number  $Sc$  and chemical reaction parameter  $\gamma$  on concentration profile is seen in Figures 17 and 18 respectively. The influence of Schmidt number on concentration is similar to that of Prandtl number on Temperature. Increase in  $Sc$  causes reduction in concentration and its boundary. Increasing the chemical reaction causes reduction in the concentration profile. The effect of increasing magnetic field parameter on temperature profile is seen on Figure 19. As  $M$  increases, temperature profile decreases. Figures 17 and 18 were plotted for the velocity and temperature profiles with variation of time using the default values. It was observed that the velocity and temperature of the fluid increases as the time increases towards a steady state

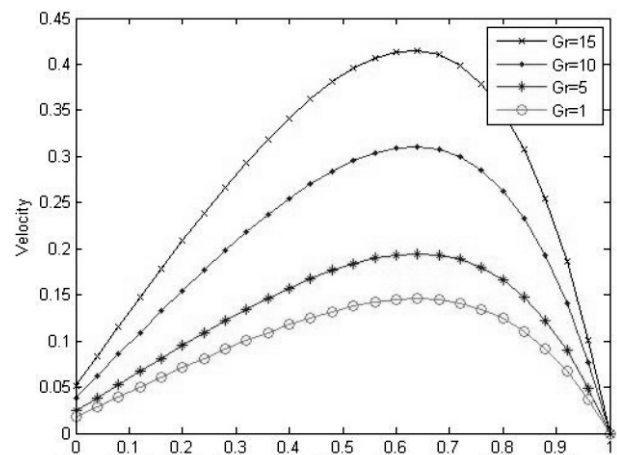


Figure 3: Velocity Profile for various Values of Thermal Grashof Number  $Gr$  at  $t=1.0$

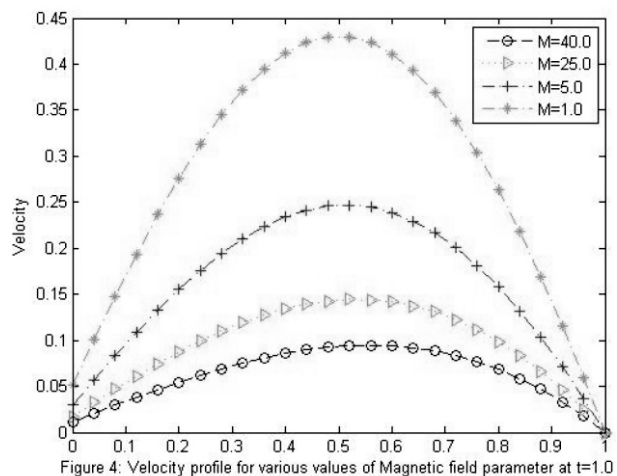


Figure 4: Velocity profile for various values of Magnetic field parameter at  $t=1.0$

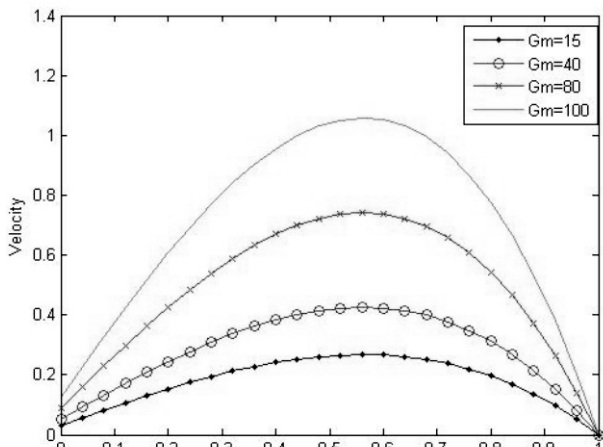


Figure 5: Velocity Profile for various values of Species Grashof number  $G_m$  at  $t=1$

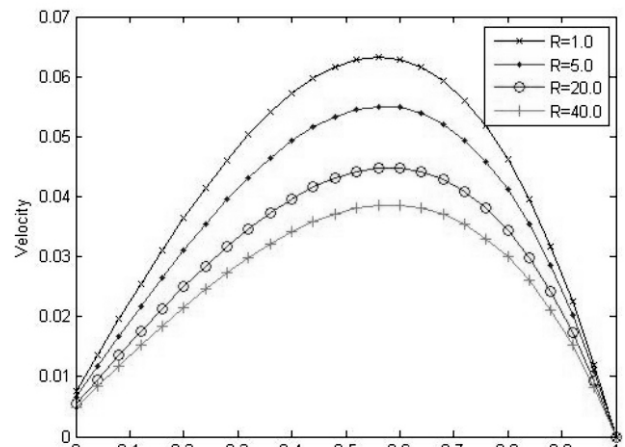


Figure 6: Velocity Profile for various values of Radiation Parameter  $R$  at  $t=1$

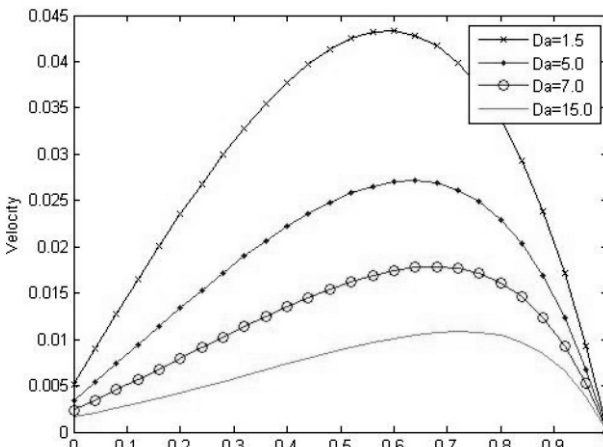


Figure 7: Velocity Profile for various values of Darcy number  $Da$  at  $t=1$

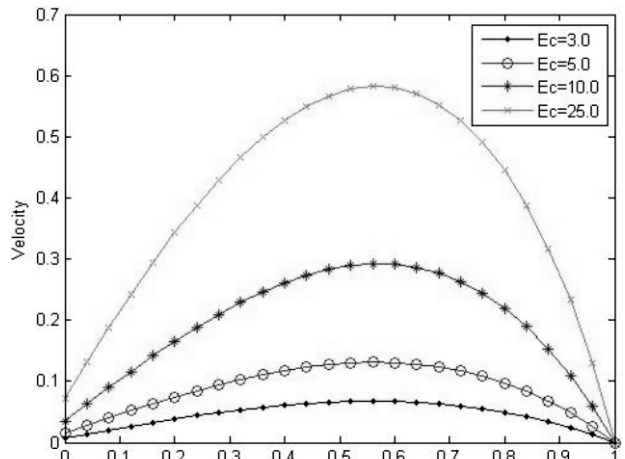


Figure 8: Velocity Profile for various values of Eckert number  $Ec$  at  $t=1$

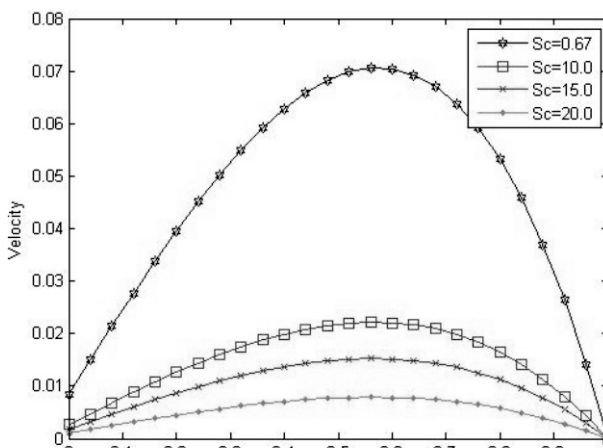


Figure 9: Velocity Profile for various values of Schmidt number  $Sc$  at  $t=1$

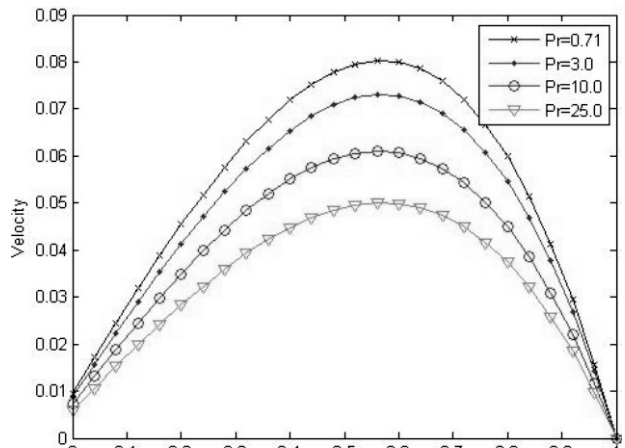


Figure 10: Velocity Profile for various values of Prandtl number  $Pr$  at  $t=1$

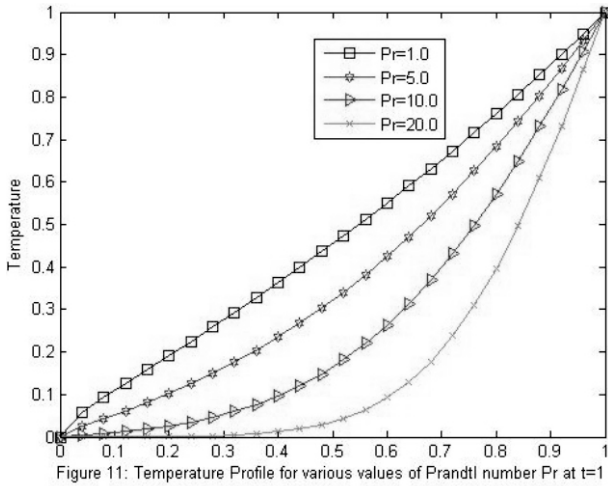


Figure 11: Temperature Profile for various values of Prandtl number  $Pr$  at  $t=1$

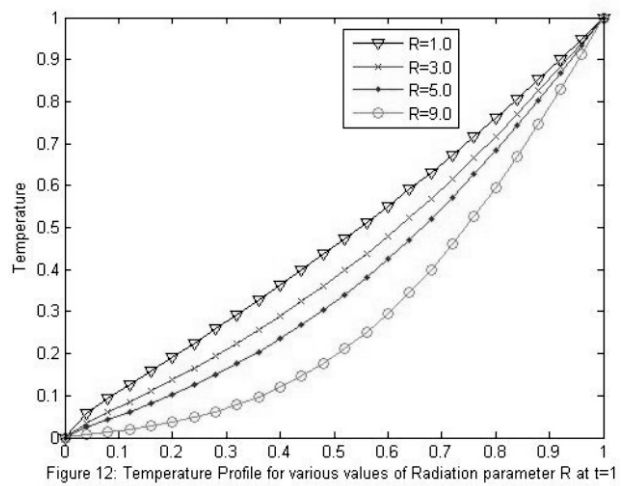


Figure 12: Temperature Profile for various values of Radiation parameter  $R$  at  $t=1$

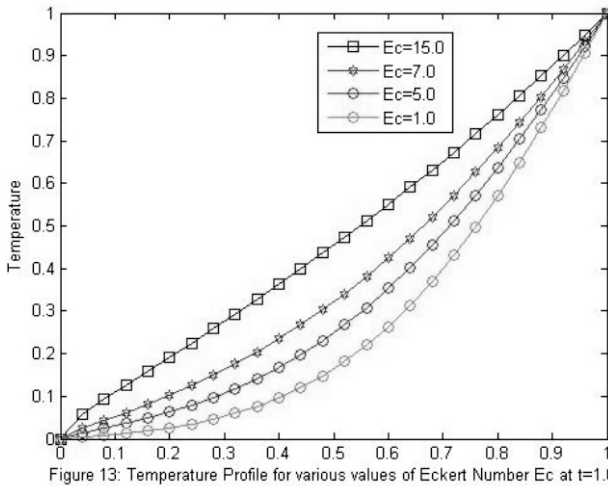


Figure 13: Temperature Profile for various values of Eckert Number  $Ec$  at  $t=1.0$

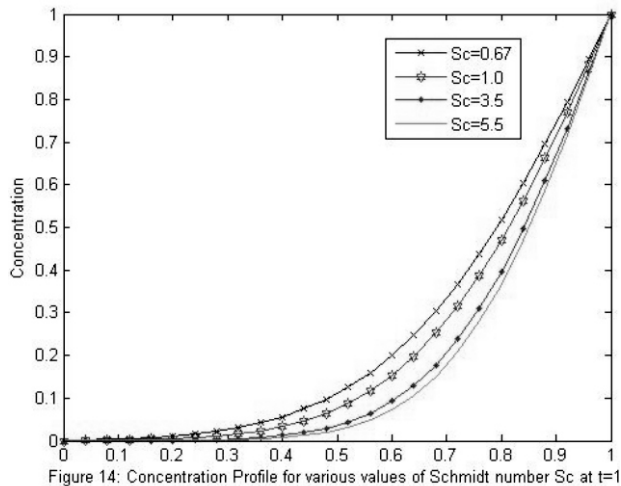


Figure 14: Concentration Profile for various values of Schmidt number  $Sc$  at  $t=1$

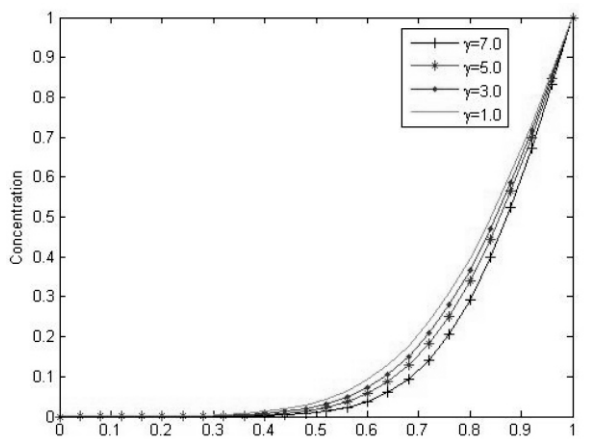


Figure 15: Concentration Profile for various values of chemical reaction parameter  $\gamma$  at  $t=1$

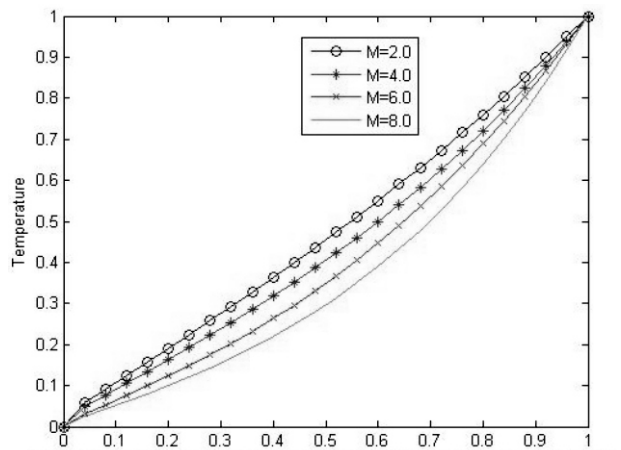


Figure 16: Temperature Profile for various values of Magnetic field parameter at  $t=1.0$

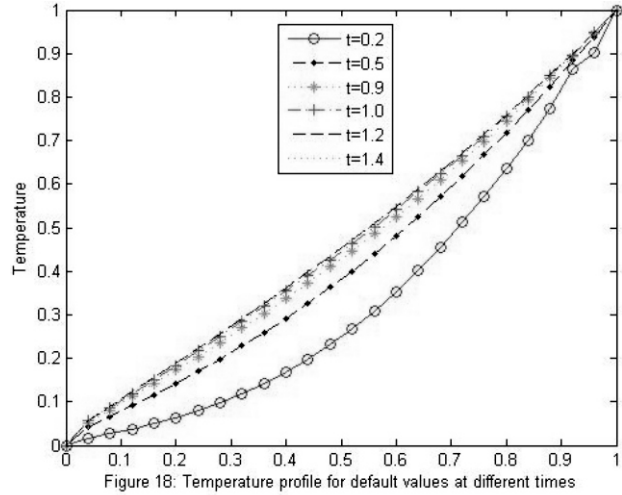
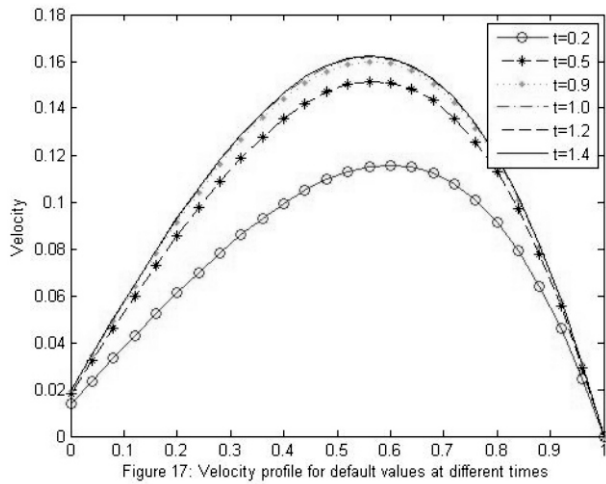


Figure 1: Variations of Skin Friction, Nusselt and Sherwood Numbers

Fluid Parameters	Skin Friction( $\tau$ )	Nusselt Number(Nu)	Sherwood Number(sh)
A=2.00	-1.6348	-0.0058	-0.0195
A=4.00	-0.5333	-0.0045	-0.0054
A=6.00	-0.2055	-0.0043	-0.0001
F=0.10	-0.4339	-0.0182	-0.0226
F=10.0	-0.4420	-0.2272	-0.2582
F=20.0	-0.4861	-0.2277	-0.2584
Gr=0.90	-0.2939	-0.0182	-0.0226
Gr=20.0	-0.3638	-0.0194	-0.0226
Gr=30.0	-0.4319	-0.0196	-0.0226
Gm=0.10	-0.2101	-0.0182	-0.0293
Gm=15.0	-0.7248	-0.0122	-0.0054
Gm=50.0	-0.7988	-0.0089	-0.0001
Ec=0.002	-0.5785	-0.0201	-0.0219
Ec=3.00	-0.6334	-0.0597	-0.0226
Ec=9.00	-0.7795	-0.1523	-0.0245
Da=0.007	-0.4274	-0.0182	-0.0235
Da=5.00	-0.3806	-0.0182	-0.0226
Da=15.00	-0.0778	-0.0182	-0.191
R=5.00	-0.3349	-0.0049	-0.0019
R=7.00	-0.3118	-0.0030	-0.0019
R=10.00	-0.0413	-0.0001	-0.0019
Sc=0.67	-0.5939	-0.0201	-0.0226
Sc=5.00	-0.3411	-0.0039	-0.0227
Sc=10.00	-0.3148	-0.0024	-0.0002
Pr=0.65	-0.3626	-0.0088	-0.0057
Pr=7.00	-0.1921	-0.0014	-0.0036
Pr=15.00	-0.1808	-0.0000	-0.0019
M=2.00	-0.2341	-0.0073	-0.0146
M=4.00	-0.1668	-0.0048	-0.0080
M=6.00	-0.0985	-0.0046	-0.0011
$\gamma$ =1.00	-0.5300	-0.0122	-0.0054
$\gamma$ =5.00	-0.2329	-0.0027	-0.0003
$\gamma$ =7.00	-0.1455	-0.0008	-0.0000

### CONCLUSION

The study considers the effect of magnetic field, thermal radiation and viscous dissipation on the problem of transient magneto hydrodynamic flow of non-Newtonian fluid in porous medium. The non-Newtonian fluid model used for describing the non-linear relationship between shear stress and rate of deformation is the Eyring-Powell model. The governing equations were formulated and transformed into non-dimensional equations. Numerical solution to the transformed governing nonlinear partial differential equations was obtained using the implicit finite difference scheme of Crank-Nicolson type. The finite difference equations form Thomas algorithm tri-diagonal matrix system of equations which was solved with the help of MATLAB. The results showed that a rise in Non-Newtonian parameter  $F$ , thermal Grashof number  $Gr$ , modified Grashof number  $Gm$  and dissipation function  $Ec$  causes velocity to increase whereas velocity decreases with increase in Non-Newtonian parameter  $A$ , magnetic field parameter  $M$ , radiation parameter  $R$ , Schmidt number  $Sc$ , Prandtl Number  $Pr$  and chemical reaction parameter  $\gamma$ . The temperature increases with increase in dissipation function  $Ec$  while it decreases as Prandtl number, magnetic field parameter and Radiation number increases. Increase in Schmidt number and chemical reaction results to a decrease in concentration.

### REFERENCES

Adesanya, S.O. and Gbadeyan, J.A. 2011. Adomia Decomposition approach to steady visco-elastic flow with slip through a planar

- channel. *Journal of Nonlinear Science* 11(1): 86-94.
- Asmat, A., Najeeb, A.K., Hassam, K. and Faqiha, S. 2014. Radiation effect on boundary layer flow of an Eyring-Powell fluid over an exponentially shrinking sheet. *Ain Shams Engineering Journal* 5, 1337-1342.
- Bird R.B., Stewart W.E and Lightfoot E.M. 1960. *Transport Phenomena*, John Wiley and Sons, New York.
- Carnahan, B., Luther, H.A., and Willkes, J.O. 1969. *Applied Numerical Method*. John Wiley and Sons, New York.
- Cogley, A.C., Vincentine, W.C. and Gilles, S.E. 1968. Differential approximation for radiative transfer in a non-gray new equilibrium. *ALAA Journal* 6, 551-555.
- Darji, R.M. and Timol, M.G. 2013. Group-Theoretic Similarity Analysis for Natural Convection Boundary Layer Flow of a Class of Non-Newtonian Fluids. *International Journal of Advanced Scientific and Technical Research* 3(1): 54-69.
- Eldaebe, N.T.M., Hassan, A.A. and Mona, A.A. 2003. Effect of couple stresses on the MHD of a non-Newtonian unsteady flow between two parallel porous plates. *Journal of physics* 58a, 204-210.
- Gbadeyan, J.A. and Dada, M.S. 2013. On the Influence of radiation and heat transfer on an unsteady MHD Non-Newtonian fluid flow with slip in a porous medium. *Journal of Mathematical Research* 5(3): 40-49.
- Hayat, T., Iqbal, Z., Qasim, M. and Obaidat, S. 2012. Steady flow of an Eyring Powell fluid over a moving surface with convective boundary conditions. *International. Journal of Heat and Mass Transfer* 55, 1817-1822.
- Islam, S., Shah, A., Zhou, C.Y. and Ali, I. 2009. Homotopy perturbation analysis of slider bearing with Powell-Eyring fluid. *Z. Angew. Math. Phys.*, 60, 1178-1193.
- Malik, A.Y., Hussian, A. and Nadeem, S. 2013. Boundary layer flow of an Eyring-Powell model fluid due to a stretching cylinder with a variable viscosity. *Journal of Scientia Iranica* 20(2): 313-321.
- Manisha, P. and Timol, M.G. 2009. Numerical treatment of Powell-Eyring fluid flow using method of satisfaction of Asymptotic Boundary conditions. *Journal of Applied Numerical Mathematics*, 59, 2584-2592.
- Mansutti, D., Pontrelli, G. and Rajagopal, K.R. 1993. Steady flow of a non-Newtonian fluids past a porous plate with suction or injection. *International Journal of Numerical Method Fluids* 17, 929-941.
- Nabil, T.M.E., Sallam, N.S. and Mohamed Y.A. 2012. Numerical study of viscous dissipation effect on free convection heat and mass transfer of MHD non-Newtonian fluid flow through a porous medium. *Journal of the Egyptian Mathematical Society* 20, 139-151.
- Patel, M. and Timol, M.G. 2009. Numerical treatment of Powell-Eyring fluid flow using method of asymptotic boundary conditions. *Appl. Numer. Math.* 59, 2584-2592.
- Patel, M. and Timol, M.G. 2011. Numerical treatment of MHD Powell-Eyring fluid flow using method of satisfaction of asymptotic boundary conditions. *Int. J. Math. Sci. Comput.* 2, 71-78.
- Tasawar, H., Sadia, A., Maraj, M. and Ahmed, A. 2014. Radiation effects on the flow of Powell Eyring fluid past an unsteady inclined stretching sheet with non-uniform Heat Source/Sink. *PLOS ONE* 9(7): e103214. doi:10.1371/journal.pone.0103214.